

Different autonomous myogenic cell populations revealed by ablation of Myf5-expressing cells during mouse embryogenesis

Nicole Gensch^{1,*}, Thilo Borchardt^{1,*}, Andre Schneider¹, Dieter Riethmacher² and Thomas Braun^{1,†}

The development of myogenic cells is mainly determined by expression of two myogenic factors, Myf5 and Myod1 (MyoD), which genetically compensate for each other during embryogenesis. Here, we demonstrate by conditional cell ablation in mice that Myf5 determines a distinct myogenic cell population, which also contains some Myod1-positive cells. Ablation of this lineage uncovers the presence of a second autonomous myogenic lineage, which superseded Myf5-dependent myogenic cells and expressed Myod1. By contrast, ablation of myogenin-expressing cells erased virtually all differentiated muscle cells, indicating that some aspects of the myogenic program are shared by most skeletal muscle cells. We conclude that Myf5 and Myod1 define different cell lineages with distinct contributions to muscle precursor cells and differentiated myotubes. Individual myogenic cell lineages seem to substitute for each other within the developing embryo.

KEY WORDS: Skeletal muscle, Cell ablation, Myf5, Myogenic cell lineages

INTRODUCTION

The formation of skeletal muscle cells during myogenesis is initiated in somites, segments of paraxial mesoderm that form in an anterior-posterior pattern on either side of the neural tube. Immature somites differentiate into dermomyotome, which generates skeletal muscle and dermal cells, and sclerotome, which is the origin of ribs and vertebrae (Arnold and Braun, 2000). Myogenic progenitor cells become restricted to the epithelium of the dermomyotome when somites mature (Buckingham, 2006). After delamination of cells from the dermomyotomal layer, myogenesis starts by stable expression of the myogenic regulatory factor (MRF) Myf5 followed by expression of myogenin, Myf6 (also called MRF4) and finally Myod1 (Neuhaus and Braun, 2002). Specification, proliferation and terminal differentiation of skeletal muscle cells is controlled by the combinatorial activities of MRFs, which, together with the paired domain transcription factors Pax3 and Pax7, are essential for skeletal myogenesis (Buckingham, 2006; Neuhaus and Braun, 2002).

We have shown previously that combined inactivation of Myf5 and MyoD mice causes a complete lack of skeletal muscle formation (Rudnicki et al., 1993), while inactivation of Myf5 and Myod1 alone results in the absence of the first wave of muscle cells (Myf5); (Braun et al., 1992) or in a moderate muscle phenotype (Myod1) (Megeney et al., 1996). More recently, it has been demonstrated that the original inactivation of the Myf5 gene also compromises expression of Myf6 at early developmental stages and that Myf6 partially rescues embryonic myogenesis in a new strain of Myf5/Myod1 double-knockout mice (Kassar-Duchossoy et al., 2004), although fetal myogenesis was severely compromised and other new strains of Myf5/Myod1 double-mutant mice were also essentially devoid of skeletal muscle at birth (Kaul et al., 2000).

The absence of lasting muscle abnormalities in mice lacking either Myf5/Myf6 or Myod1, and the complete lack of skeletal muscle cells in compound Myf5/Myf6/Myod1 mutant mice suggested that MRFs play functionally overlapping roles during muscle cell development. In order to distinguish whether Myf5/Myf6 and Myod1 substitute for each other within the same cell lineage or whether, alternatively, each factor determines a distinct muscle cell population we previously ablated Myf5-expressing cells in ES-cell derived skeletal muscle cells using a HSV thymidine suicide gene inserted into the Myf5 locus (Braun and Arnold, 1996). Although we were able to demonstrate that complete ablation of Myf5-expressing muscle precursor cells from differentiating ES cells does not abrogate Myod1-dependent muscle cell differentiation in vitro (Braun and Arnold, 1996), the nature of compensation between *Myf5/Myf6* and *Myod1* genes has been questioned. In particular, it has been claimed that Myf5 acts upstream of Myod1, as Myod1 expression in somites was delayed until after E10.5 in Myf5^{nlacZ/nlacZ} embryos (Tajbakhsh et al., 1997). This statement was later modified, as Myod1 expression was detected before E10.5 in Myf5 mutants, in which Myf6 expression was not compromised (Kassar-Duchossoy et al., 2004; Kaul et al., 2000). The existence of parallel cell lineages determined by individual bHLH genes has also been demonstrated in the nervous system where Ngn2 and Ngn1 determine two genetically and lineally distinct populations of sensory neuron precursors, which can be both independently regulated in distinct sensory lineages, as well as crossregulated within a given lineage. The neurogenesis defect in Ngn2 mutant embryos is transient (as in Myf5 mutant mice) and later compensated for by Ngn1-dependent precursors, suggesting that feedback or competitive interactions between these precursors may control the proportion of different neuronal subtypes they normally produce (Ma et al., 1999).

To demonstrate that Myf5 is expressed only in a distinct population of muscle precursor cells and hence determines only a subset of muscle cells, we have employed an in vivo conditional cell ablation approach based on activation of the diphtheria toxin A-chain (DTA) by Cre-recombinase. Activation of DTA in Myf5-Cre-expressing cells erased all Myf5-expressing cells until E15.5, which included the majority of early muscle cells in somites. Ablation of

¹Max-Planck-Institute for Heart and Lung Research, Parkstr. 1, 61231 Bad Nauheim, Germany. ²Human Genetics Division, University of Southampton, Southampton SO16 6YD, UK.

*These authors contributed equally to this work

[†]Author for correspondence (e-mail: thomas.braun@mpi-bn.mpg.de)

early muscle cells was fully rescued by another, Myf5-independent, cell population, demonstrating initiation of the muscle program in autonomous cell populations. Interestingly, however, later aspects of the myogenic program are shared among all populations of muscle cells as the ablation of myogenin-expressing cells erased virtually all differentiated muscle cells at E18.5. We also detected malformations of the axial skeleton in Myf5-Cre/DTA mice, which might be due to transient activation of the Myf5 gene in the unsegmented paraxial mesoderm.

MATERIALS AND METHODS

Origin of mouse mutants

The generation of Myf5-Cre mice, (Tallquist et al., 2000), of the Rosa26lacZ Cre-reporter strain (Soriano, 1999), of myogenin-Cre mice (Li et al., 2005), of R26:lacZ/DTA (DTA) effector mice (Brockschneider et al., 2004) and of Z/AP reporter mice (Lobe et al., 1999) have all been described before. Mice were crossed to and maintained on a C57/BL6 background and genotyped by Southern blot analysis or PCR.

Immunofluorescence, in situ hybridization, lacZ staining and skeletal analysis

For immunofluorescence and histological staining, cryosections were prepared and processed applying standard procedures (Schulze et al., 2005; Ustanina et al., 2007). The following antibodies were used: MF20 (DSHB), anti-myogenin (DSHB), anti-Myf5 (Santa Cruz), anti-MyoD1 (clone 5.8A, Dako GbmH) and anti-Pax7 (DSHB). Secondary antibodies were coupled with Alexa 594 (red) and Alexa 488 (green), and used according to the manufacturer's instructions (Molecular Probes). Whole-mount in situ hybridization with digoxigenin-labeled antisense cRNA probes and sectioning of stained embryos were performed as described previously (Schäfer and Braun, 1999). *lacZ* staining was performed as described previously (Oustanina et al., 2004). Alkaline phosphatase staining was done on cryosections using the Vector Red Alkaline Phosphatase Substrate Kit I (Cat. No. SK-5100), according to the instructions supplied by the manufacturer (Vector Labs). For bone and cartilage staining, fetuses were processed as described (Kaul et al., 2000).

RNA isolation and RT-PCR

Isolation of RNA was carried out using established procedures that have been described previously (Schulze et al., 2005; Ustanina et al., 2007). RT-PCR analysis was essentially done as described (Schulze et al., 2005). Detailed protocols and primer sequences are available from the authors on request. In all cases, housekeeping genes such as ribosomal acidic protein (RAP) or glyceraldehyde-3-phosphate dehydrogenase (GAPDH), were used as internal controls. Identities of PCR products were corroborated by DNA sequence analysis.

RESULTS

Cells with a history of Myf5 promoter activation do contribute to multiple tissues

The onset of myogenesis is defined by stable activation of the Myf5 promoter in the epaxial dermomyotome, which is followed by differentiation of Myf5-expressing cells that have migrated under the dermomyotome (Buckingham, 2006). Subsequently, several waves of muscle cells form and give rise to various muscles of the body. To investigate whether all muscle cells were derived from Myf5-expressing cells (referred to as Myf5-derived cells in this paper) or whether the Myf5 lineage contributes to the cellular heterogeneity of muscular cells, as suggested by previous experiments using ES-cell derived skeletal myocytes (Braun and Arnold, 1996), we crossed Myf5-Cre mice, which carry a Cre-recombinase inserted into the Myf5 locus (Tallquist et al., 2000), with a Rosa26lacZ Cre-reporter strain (Soriano, 1999). The same Myf5-Cre strain has been employed in a number of studies to trace Myf5-expressing cells in satellite cells of adult mice (Kuang et al.,

2007) or to delete genes in skeletal muscle (Wang et al., 2005). A strong expression of the *lacZ* reporter gene was observed at E10.5 (Fig. 1C-F). Interestingly, the expression was not only confined to the myotome but was also found in other parts of the embryo such as the dermomyotome and the sclerotome, which are derived from the paraxial mesoderm. Most likely, this expression was due to a transient activity of the Myf5 promoter in the paraxial mesoderm, which was not detectable by direct visualization of Myf5 promoter activity (Tajbakhsh et al., 1997). To further explore this possibility, we performed a RT-PCR analysis of the expression of MRFs in the paraxial mesoderm and the head of E8.5 embryos. After 35 amplification cycles, we detected an expression of Myf5 in the unsegmented paraxial mesoderm but not in the head region (see Fig. S1 in the supplementary material). A very faint signal was also found for Myf6 but not for MyoD1 and myogenin.

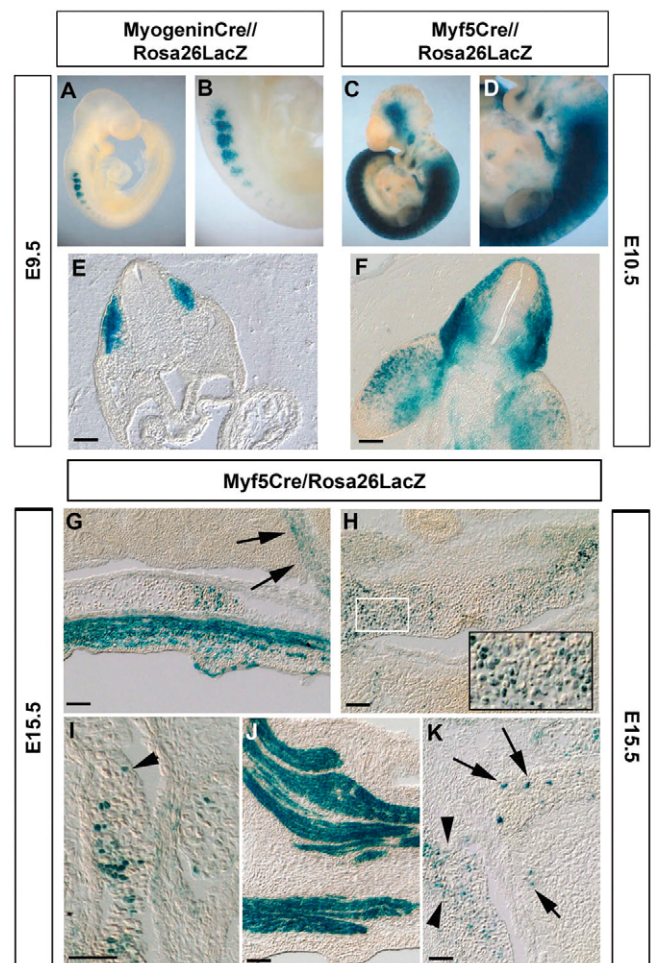


Fig. 1. Contribution of Myf5-derived cells to different cell types of the paraxial mesoderm. (A-K) Expression of *lacZ* in E9.5 (A,B,E), E10.5 (C,D,F) and E15.5 (G-K) Rosa26lacZ embryos crossed either with myogenin-Cre (A,B,E) or with Myf5-Cre mice (C,D,F-K). *lacZ* staining (blue) reveals Myf5-derived cells in the sclerotome at E10.5 (F), in the rib cartilage (G,I), vertebrae (H) and skeletal muscles of the body wall (G) and of a limb (J). Arrows in G indicate the limited presence of Myf5-derived cells in the diaphragm of this embryo. Very few Myf5-derived cells are present in the neural tube and in the dorsal root ganglia (arrows in K). Arrowheads in K indicate *lacZ*-positive chondrocytes in a vertebra. Scale bars: 100 μ m.

We also observed numerous *lacZ*-positive cells in the neural tube and the brain (data not shown), which corroborates previous reports about the activity of the *Myf5* gene during embryogenesis (Tajbakhsh and Buckingham, 1995; Tajbakhsh et al., 1994). Five days later, at E15.5, most *lacZ*-positive cells were located within skeletal muscle masses of the trunk, head and limbs (Fig. 1G,J and data not shown), although some *lacZ*-positive cells were also found in cartilage cells of the axial skeleton (ribs and vertebrae) and in the dermis, which reflects their origin from the paraxial mesoderm (Fig. 1). Only relatively few *lacZ*-positive cells remained in tissues derived from the neural tube (Fig. 1K), suggesting an active removal of *Myf5*-derived cells from certain tissues. Surprisingly, the distribution of *Myf5*-derived cells among different muscles varied. In some muscles, the majority of muscle cells were labeled, while in other muscles (as for example the diaphragm) the contribution was limited (arrows in Fig. 1G and data not shown). We also noted significant differences in the contribution of *Myf5*-derived cells to separate muscles among individual mice, suggesting that the distribution of *Myf5*-derived cells was controlled by a stochastic mechanism. We did not find evidence for an increased presence of *Myf5*-lineage derived cells in autochthone muscles of the back or in limb muscles, which argues against a specific role of *Myf5*-expressing cells in the formation of epaxial and hypaxial muscles.

In contrast to *Myf5*, the myogenic regulatory factor myogenin is expressed later during somitic development and has been demonstrated to play a crucial role in the differentiation of embryonic myoblasts into myocytes. Myogenin-derived cells should identify all skeletal muscle cells as myogenin-null mice lack differentiated skeletal muscle fibers, thereby demonstrating that myogenin is absolutely required for embryonic muscle differentiation and has no redundant or compensatory mechanisms to replace its function (Hasty et al., 1993). Breeding of myogenin-Cre mice (Li et al., 2005) with a *Rosa26lacZ* Cre-reporter strain (Soriano, 1999) led to *lacZ* expression in the myotome of the most mature somites at E9.5 (Fig. 1A,B). At E15.5 virtual all muscle cells were positive for *lacZ* (see Fig. S2 in the supplementary material), confirming the indispensable role of myogenin for embryonic muscle differentiation.

The myogenic lineage is established from multiple independent muscle progenitor populations

Previously, we have demonstrated that ablation of *Myf5*-expressing muscle precursors cells did not prevent *MyoD1*-dependent muscle cell differentiation. The system employed was based on ES cells engineered to carry the HSV TK suicide gene in one allele and the *lacZ* reporter gene in the other allele of the *Myf5* gene (Braun and Arnold, 1996). Although ES cell-derived skeletal myoblasts offer some experimental advantages they lack the complexity of normal embryonic development. In addition, more subtle changes in the spatial and temporal distribution of myogenic cell populations might be obscured in the *in vitro* model (Braun and Arnold, 1994). We therefore turned to an *in vivo* cell ablation system that uses Cre-recombinase-mediated activation of the diptheria toxin A-chain (DTA). To examine the efficiency of DTA-mediated elimination of *Myf5*-derived cells, we crossed *Myf5*-Cre mice to *Z/AP* reporter mice, which activate the alkaline reporter gene instead of the *lacZ* reporter gene upon Cre-recombinase-mediated recombination (Lobe et al., 1999). The use of *Z/AP* mice was necessary as our *R26/lacZ/DT-A* (DTA) effector mice express *lacZ* ubiquitously (Brockschneider et al., 2004). At E15.5, skeletal muscles were labeled by AP activity (Fig. 2A,C,E) comparable with *Myf5*-

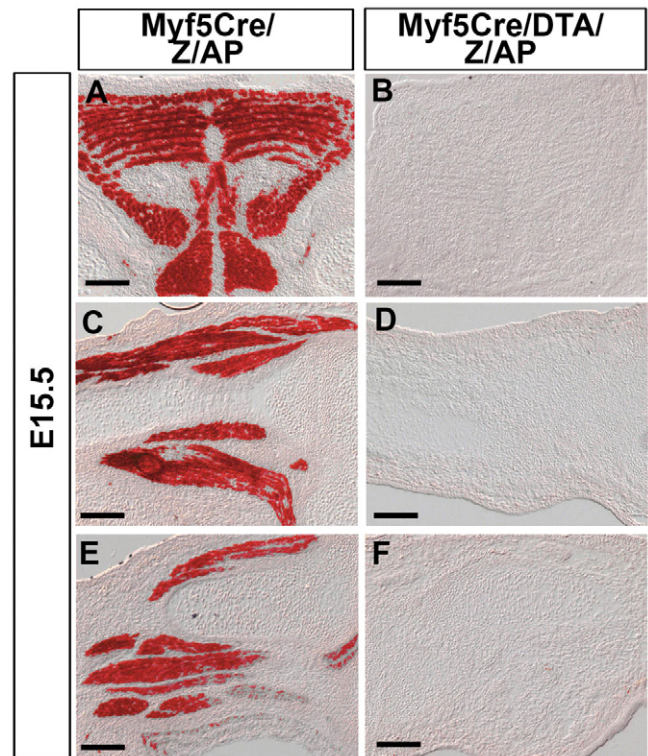


Fig. 2. Efficient DTA-mediated ablation of *Myf5*-derived cells at E15.5. *Myf5*-Cre mice were crossed either to *Z/AP* reporter mice (A,C,E) or to *Z/AP/DTA* mice (B,D,F). AP staining (red) reveals *Myf5*-derived cells in different muscles of *Myf5*-Cre/*Z/AP* mice at E15.5 (A,C,E). Simultaneous activation of DTA by *Myf5*-Cre leads to a complete ablation of *Myf5*-derived cells in *Myf5*-Cre/*DTA/Z/AP* mice (B,D,F). (A,B) tongue muscles. (C-F) Limb and body wall muscles. Scale bars: 200 μ m.

Cre/*Rosa26lacZ* mice. We next crossed *Myf5*-Cre/*Z/AP* mice to *R26/lacZ/DT-A* (DTA) mice and found that *Myf5*-Cre/*DTA/Z/AP* embryos were essentially devoid of any *Myf5*-derived cell at E15.5, as indicated by the absence of AP-positive cells (Fig. 2B,D,F).

Similar to *Myf5*-Cre/*Rosa26lacZ* mice, we observed variations in the distribution of *Myf5*-derived cells among different muscles, suggesting that this phenomenon was not due to a variable expression from the *Rosa26lacZ* or from the unrelated *Z/AP* locus. Interestingly, mice lacking *Myf5*-derived cells did not show a significant loss of muscle masses, as judged from differential interference contrast microscopy (Fig. 2B,D,F). Immunofluorescence analysis of muscles of *Myf5*-Cre/*DTA* mice at E14.5 and E18.5 using an antibody against MyHC (MF-20) confirmed the normal formation of skeletal muscles in the absence of *Myf5*-derived myogenic cells (Fig. 3A,D,G,J). By contrast, myogenin-Cre/*DTA* mice failed to form differentiated muscle at E18.5 (Fig. 3E,H,K). The formation of essentially normal skeletal muscles at E18.5 in *Myf5*-Cre/*DTA* and the loss of muscles masses in myogenin-Cre/*DTA* at this stage were also confirmed by inspection of Hematoxylin and Eosin-stained tissues sections (see Fig. S3 in the supplementary material). Efficient killing of muscle cells in myogenin-Cre/*DTA* mice was not apparent before E14.5, indicating a considerable delay between the onset of promoter activity that drove Cre-recombinase expression, recombination of the DTA locus and DTA-mediated cell death (Fig. 3B and data not shown).

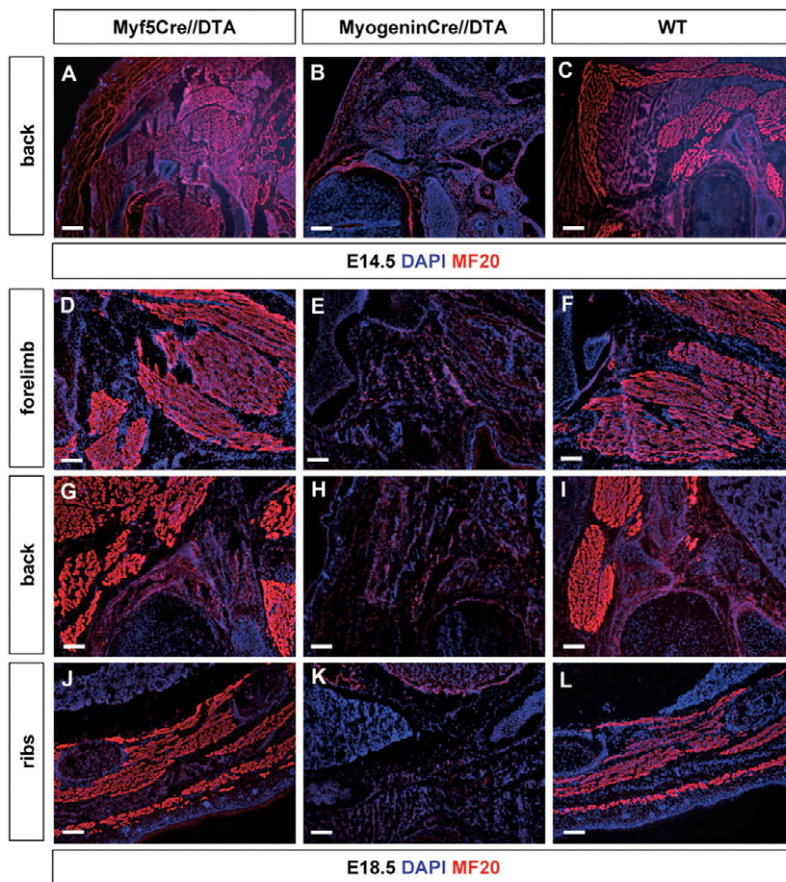


Fig. 3. Loss of MyHC-expressing skeletal muscle cells in myogenin-Cre/DTA mice at E18.5.

(A-L) Immunofluorescence staining with a MyHC antibody (MF20) of sections from Myf5-Cre/DTA (A,D,G,I), myogenin-Cre/DTA (B,E,H,K) and wild-type mice (C,F,I,L) at E14.5 (A-C) and E18.5 (D-L). Note the absence of MyHC-positive muscle cells in myogenin-Cre/DTA but not in Myf5-Cre/DTA mice, which show a virtually normal formation of skeletal muscles at E18.5. Sections from wild-type mice are shown for comparison. Scale bars: 200 μ m.

Clearly, embryos were able to compensate for the ablation of Myf5-derived cells to form normal skeletal muscles but not for the absence of cells that had expressed myogenin. This finding was also supported by a preliminary DNA microarray-based analysis of Myf5-Cre/DTA E14.5 embryos using the GeneChip Mouse Genome 430 2.0 Array (Affymetrix). Only very few structural muscle genes were significantly changed in Myf5-Cre/DTA mice compared with wild-type controls, indicating a relatively normal formation of skeletal musculature (see Table S1 in the supplementary material). The complete dataset of the microarray experiment has been deposited in the ArrayExpress repository (Accession Number E-MEXP-1486). Apparently, muscle cells that developed from non-Myf5-derived cells generated a similar expression profile to Myf5-derived cells, which suggested a similar developmental potential of Myf5-derived and non-Myf5-derived muscle progenitor cells. The DNA microarray analysis also revealed a decrease of Myf5 expression and a reduction of the expression of Myf6 of a log ratio of 1.8. Owing to the low expression level of Myf5 at E14.5, the decline of Myf5 expression appeared comparatively modest (see Table S1 in the supplementary material).

We next investigated the effects of the ablation of Myf5-derived cells on the expression of other myogenic regulatory factors that might mark parallel myogenic cell lineages by RT-PCR. At E10.5, we found a severe downregulation of Myf5-expression, reflecting the loss of Myf5-expressing cells. Surprisingly, we also observed a strong downregulation of Myod1 and myogenin and to a lesser degree of Myf6 in Myf5-Cre/DTA mice at E10.5, while the global expression level of Pax3 and Pax7 was not significantly affected (Fig. 4). At E14.5, the expression of Myod1 returned to control

levels and the expression of myogenin and Myf6 was only mildly affected, which was in agreement with the DNA microarray analysis.

Immunofluorescence analysis of Myf5-Cre/DTA, myogenin-Cre/DTA and wild-type mice at E10.5 revealed a complete loss of cells that expressed Myf5 protein (Fig. 5A,D,G). The ablation of Myf5-expressing cells was already starting 1 day earlier at E9.5, as indicated by the significant reduction of the number of cells that stained positive for Myf5 protein, although some remaining cells were clearly visible at this stage (see Fig. S4 in the supplementary material). At E10.5, we also observed a massive reduction of the number of Myod1 and myogenin-expressing cells, which occurred concomitant with the loss of Myf5-positive cells (Fig. 5A,D,G). The remaining Myod1 and myogenin-positive cells were scattered within the somites (Fig. 5A,G), which had lost their regular architecture (Fig. 5A,D,G). Pax7-positive cells were found only at the dorsolateral and ventromedial edges of the dermomyotome, while the central area was devoid of Pax7 expression (Fig. 5D). The induction of cell death by Cre recombinase-mediated activation of DTA was also accessed directly using the TUNEL assay. We detected a large number of TUNEL-positive apoptotic cells in somites of Myf5-Cre/DTA mice at E9.5 and E10.5, but only a comparatively small number of apoptotic cells was present in somites of wild-type mice (see Fig. S5 in the supplementary material). No reduction of Myf5, myogenin, Myod1 or Pax7 was observed in myogenin-Cre/DTA embryos at E10.5, which corresponds to the later onset of expression of the myogenin-Cre and the activity of the myogenin-promoter in differentiating muscle cells. Similar to the

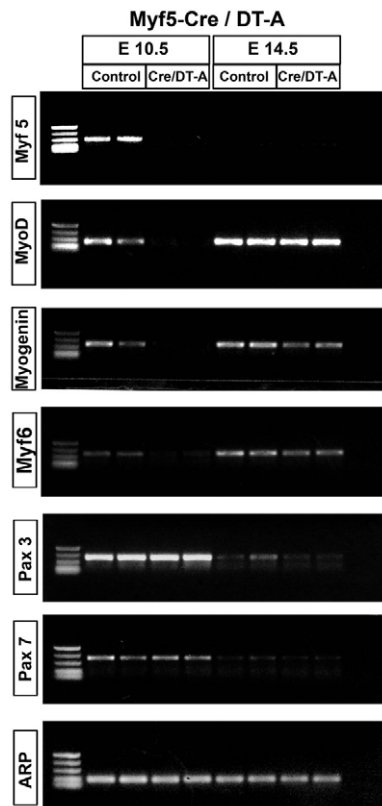


Fig. 4. Reduced expression of MRFs in Myf5-Cre//DTA mice at E10.5. Semi-quantitative RT-PCR analysis of Myf5, MyoD, myogenin, Myf6, Pax3 and Pax7 mRNAs from E10.5 and E14.5 wild-type and Myf5-Cre/DTA mice. Acidic ribosomal protein (ARS) served as a loading control.

loss of cells that stained positive for Myf5 protein, using RNA in situ hybridization we observed a loss of cells that expressed Myf5 mRNA at E10.5 in cranial somites (see Fig. S6B in the supplementary material). In the caudal part of Myf5-Cre//DTA embryos, residual amounts of Myf5 mRNA-positive cells were still detectable (see Fig. S6H in the supplementary material) reflecting the ongoing process of cell ablation, which was completed only at E15.5 (Fig. 2). Similarly, no mRNAs for MyoD1 and myogenin were detected in cranial somites at E10.5 (see Fig. 6D,F in the supplementary material), although some signals were present in caudal somites (see Fig. S6J,L in the supplementary material). The localization of signals in caudal somites was aberrant, again reflecting the continuing process of cell death and the resulting disorganization of the somites. In our view, the persistent presence of some dislocated Myf5 transcripts within somites of Myf5-Cre//DTA embryos (see Fig. S6H in the supplementary material) in the absence of Myf5 protein reflects the delay between the onset of Myf5-Cre-, Cre-recombinase-mediated DTA activation and cell death.

The relatively normal appearance of the skeletal musculature of Myf5-Cre//DTA embryos at E14.5 and E18.5 was most probably due to a compensatory increase of myogenic cells, which express MyoD1 but not Myf5. To explore this possibility, we analyzed the expression of MyoD1 in Myf5-Cre//DTA and wild-type embryos. We detected a strong increase of the expression of MyoD1 in Myf5-Cre//DTA embryos between E11.5 and E12.5 (Fig. 6B,C). At E11.5, the expression of MyoD1 was mostly confined to the hypaxial part

of somites, which is still highly abnormal. One day later, however, at E12.5 the differences between wild-type and Myf5Cre//DTA mice were only minor (Fig. 6C,F). Apparently, MyoD1-dependent cells underwent an accelerated proliferation to fill the gap created by the Myf5 ablation.

Myf5-Cre//DTA mice die perinatally due to severe malformations of the axial skeleton

Both Myf5-Cre//DTA and myogenin-Cre//DTA were born at normal Mendelian ratios but died shortly after birth. Although we expected this outcome for myogenin-Cre//DTA mice, which lacked all skeletal muscles at E18.5, the perinatal death of Myf5-Cre//DTA, which did not show any major alterations of the skeletal musculature at E18.5, was a surprise. As we observed the presence of Myf5-derived *lacZ*-positive cells in the cartilage of the axial skeleton at E15.5 (Fig. 1G,H), we decided to analyze the skeleton of newborn Myf5-Cre//DTA mice by Alcian Blue/Alizarin Red staining. We detected major deformities of the axial skeleton, including fusion of ribs and vertebrae, lack of distal and proximal parts of the ribs and other defects (Fig. 7). In general, the observed malformation were variable and severe, thus differing from the stable phenotype, which we have observed previously in Myf5 mutant mice and which always affected only the distal parts of the ribs (Braun et al., 1992).

DISCUSSION

The Myf5-Cre//Rosa26lacZ mice revealed that more cells than previously anticipated were derived from Myf5-expressing cells. Previous reports, which were based on in situ hybridization (Ott et al., 1991) and a direct knock-in of the *lacZ* reporter into the Myf5 locus (Tajbakhsh et al., 1996a) showed a much more restricted expression pattern of Myf5, which reflects the difference between permanent cell tracing and temporarily restricted gene activity. Although the β -galactosidase protein is rather stable in certain cells, transient activity of a promoter might escape detection or might not suffice to generate sufficient amounts of a reporter protein. The relatively broad presence of Myf5-derived cells in tissues originating from the paraxial mesoderm and the neuroectoderm in Myf5-Cre//Rosa26lacZ embryos might be explained in two ways: (1) aberrant activity of the Myf5-Cre inserted into the Myf5 locus, which causes *lacZ*-activation in tissues derived from the paraxial mesoderm and the neural tube; or (2) transient activity of the Myf5 promoter in the paraxial mesoderm, which was not detectable by direct visualization of Myf5 promoter activity as described by Tajbakhsh et al. (Tajbakhsh et al., 1996a). The fact that Myf5-derived cells were confined to tissues of the paraxial mesoderm and the neural tube at E9.5 and E10.5, and not in uncharacteristic locations within the embryo makes an aberrant activity of Myf5-Cre at E9.5 and E10.5 unlikely. Usually, it takes 1-2 days until the recombination initiated by Cre-recombinase is completed and cell labeling occurs, which suggests that the presence of *lacZ*-positive cells at E9.5 and E10.5 was due to an activity of Myf5-Cre at earlier time points. A transient activity of the Myf5 promoter in the paraxial mesoderm around E8 would explain the observed presence of Myf5-derived cells in progeny of the paraxial mesoderm. In fact, we were able to detect a low-level expression of Myf5 in unsegmented paraxial mesoderm by RT-PCR. Similar observations were also made in our laboratory several years ago, which were neglected at that time as no further evidence for an activity of the Myf5/Myf6 locus in the unsegmented paraxial mesoderm existed (data not shown). Moreover, further evidence for an activity of the Myf5 promoter in unsegmented mesoderm comes from other species. In the zebrafish, Chen et al. have described a significant expression of

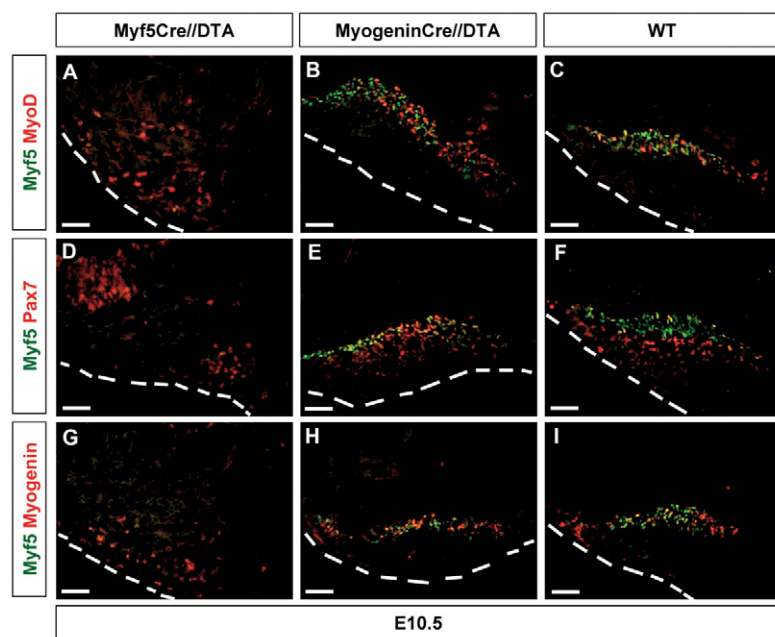


Fig. 5. Loss of Myf5-expressing cells in somites of Myf5-Cre//DTA mice at E10.5. Immunofluorescence staining of somites of Myf5-Cre//DTA (A,D,G), myogenin-Cre//DTA (B,E,H) and wild-type embryos (C,F,I) at E10.5 using a combination of Myf5 and MyoD1, Myf5/Pax7 and Myf5/myogenin antibodies. Somites from the cranial part of embryos are shown. Myf5-expressing cells are lacking in Myf5-Cre//DTA but not in myogenin-Cre//DTA and wild-type embryos, and there is a massive reduction of MyoD1- and myogenin-expressing cells in Myf5-Cre//DTA embryos. Broken lines indicate the outline of the embryos. Scale bars: 100 μ m.

Myf5 in the unsegmented paraxial mesoderm (Chen et al., 2001). It is also intriguing to see that cells that carry a homozygous mutation of the *Myf5* gene are able to contribute to other somitic derivatives, according to their local environment (Tajbakhsh et al., 1996b), including the axial skeleton and the dermis, exactly the tissues that also harbor Myf5-derived cells. In our view, this observation further supports the hypothesis that a transient activity of the Myf5 promoter occurs in multipotent cells of the paraxial mesoderm, which is later stabilized by specific positional cues

eventually leading to the characteristic Myf5 expression profile (Buckingham, 2001). Taken together, our results indicate that the activity of the Cre-recombinase inserted into the Myf5 locus faithfully recapitulates (a transient) expression of Myf5 in the paraxial mesoderm, although we cannot rule out completely that the insertion of the cre-recombinase gene into the Myf5 locus affected its regulation. The latter caveat might principally be raised for all reporter genes inserted by targeted recombination.

The activity of the Myf5 promoter in the unsegmented mesoderm does also explain the defects of the axial skeleton of Myf5-Cre//DTA mice, which are clearly due to ablation of cells in the sclerotome and sclerotome-derived cells forming the axial skeleton. As we have only used heterozygous Myf5-Cre//DTA mice in our experiments, we can rule out that the skeleton phenotype was due to cis-effects caused by the integration of the Myf5-Cre allele, which we have identified previously to be responsible for the rib anomalies in the original Myf5 mutants (Myf5^{ml}) (Kaul et al., 2000). Although the skeleton phenotypes of Myf5^{ml} and Myf5-Cre//DTA mice are caused by different effects and vary significantly between both strains, they both reveal the vulnerability of the formation of the axial skeleton. Unlike the skeletal muscle lineage (and probably dermal cells), which are able to compensate even major losses of cells, the axial skeleton seems to lack this ability. It is tempting to speculate that the compensatory potential of the skeletal muscle lineage is based on the high proliferative and migratory capacities of fetal myoblasts, a property that is also maintained throughout adult life and accounts for the exceptional regenerative capacity of skeletal muscle.

Our study clearly demonstrates that only a subset of myogenic cells expresses Myf5 and that this cell population is one among others, which form the skeletal muscle lineage. Interestingly, the Myf5-derived cell population seems not to coincide with any known myogenic cell lineage as, for example, epaxial or hypaxial cells, which have been proposed to depend differentially on Myf5 and MyoD1 (Kablar et al., 1997), and on fast or slow muscle cells (Biressi et al., 2007). This raises the question about the functional importance of Myf5-derived cells. As our previous in vitro studies using ES cell derived skeletal myoblasts suggested the existence of

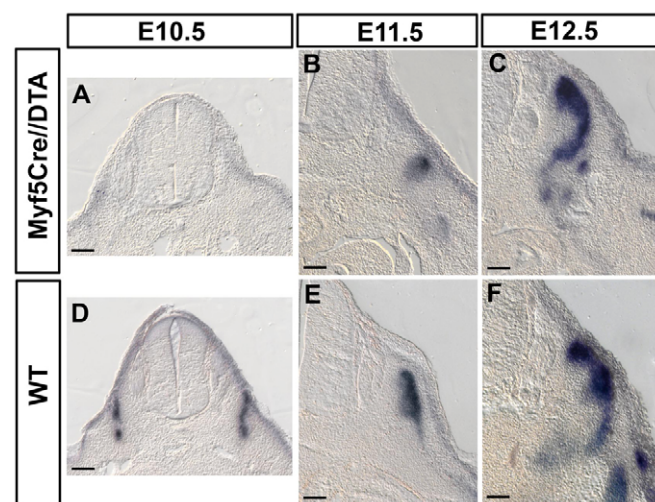


Fig. 6. Compensatory increase of MyoD1 expression in Myf5-Cre//DTA embryos. (A-F) In situ hybridization of Myf5-Cre//DTA (A-C) and wild-type (D-F) embryos at E10.5 (A,D), E11.5 (B,E) and E12.5 (C,F) with a probes against MyoD1. No expression of MyoD1 was observed in Myf5-Cre//DTA embryos at E10.5. At E11.5 an abnormal expression of MyoD1 was present in the hypaxial part of the dermomyotome of Myf5-Cre//DTA embryos compared with the more widespread expression in wild-type embryos. At E12.5, no major differences in the expression of MyoD1 were found between wild-type and mutant embryos. Scale bars: 150 μ m.

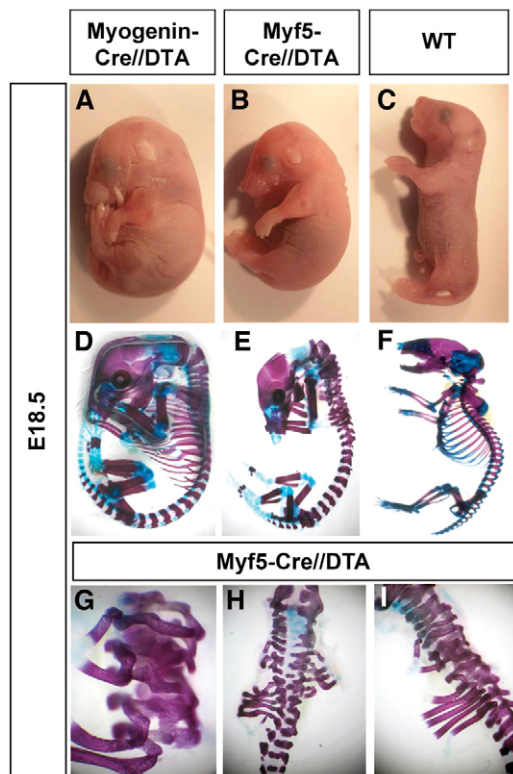


Fig. 7. Defects of the axial skeleton in Myf5-Cre//DTA mice at E18.5. (A–F) Macroscopic views of newborn myogenin-Cre//DTA (A,D), Myf5-Cre//DTA (B,E) and WT (C,F) before (A–C) and after Alizarin Blue/Alizarin Red staining (D–F). Enlarged views of the deformed skeleton of Myf5-Cre//DTA mice (G–I). Note the abnormal posture of myogenin-Cre//DTA mice, owing to the absence of skeletal muscles. No primary malformations of the skeleton of myogenin-Cre//DTA mice are apparent.

Myf5-independent muscle cell lineages, it was surprising to see that most of the early MyoD1 expressing cells were killed during early somitogenesis. These results might be explained by the activation of the MyoD1 gene in most Myf5-expressing cells, which also corresponds to the co-expression of Myf5 and MyoD1 in established muscle cell lines and at later stages of fetal skeletal muscle development. A distinct cell population, however, was obviously independent of Myf5 and expressed MyoD1. These cells, which need further characterization, allowed expansion of the myogenic cell lineage and efficient rescue of myogenesis. It is also interesting to note that the lack of the primary wave of muscle cells in Myf5 knockout mice were also compensated efficiently during embryogenesis, resulting in essentially normal musculature in adult Myf5 knockout mice (Gayraud-Morel et al., 2007; Ustanina et al., 2007). Based on the preliminary DNA microarray analysis at E14.5 and the regular formation of skeletal muscles at E18.5, the MyoD1-dependent cell lineage did not show major differences to the heterogeneous mix of cell populations that develop normally, indicating a high degree of plasticity and adaptability.

The high plasticity of skeletal muscle is also reflected by an enormous heterogeneity of skeletal muscle cells, which is not only restricted to developed fibers but also apparent during development and adult life at molecular and cellular levels, as indicated by recent cell lineage and gene expression studies (Biressi et al., 2007). Using the same Myf5-Cre strain that was employed in this study and a

ROSA26-YFP Cre-reporter strain, it has been described that 10% of sublamina Pax7-positive satellite cells did never express Myf5 (Kuang et al., 2007). As Pax7⁺/Myf5[−] satellite cells gave rise to Pax7⁺/Myf5⁺ satellite cells through asymmetric cell division, Kuang et al. argued that Pax7⁺/Myf5[−] are on top of a hierarchy of muscle stem cells that give rise to new (Pax7⁺/Myf5[−]) stem cells and to committed (Pax7⁺/Myf5⁺) myogenic progenitors. Our finding that Myf5 myogenic cells form only a subset of muscle cells, therefore contributing to the heterogeneity of muscle cells during development, raises the question whether Pax7⁺/Myf5[−] cells did indeed never see a muscle regulatory factor of the Myf5/MyoD1 family and thus belong to a more immature muscle stem cell lineage. Alternatively, it might be envisaged that Pax7⁺/Myf5[−] cells depend on other MRFs and thus do not belong to the Myf5-derived muscle cell population. The widespread presence of MyoD1-derived satellite cells in adult muscles (David Goldhammer, University of Connecticut, personal communication; N.G., T.B., A.S., D.R. and T.B., unpublished) does also argue in this direction. It will be interesting to determine whether Pax7⁺/Myf5[−] cells are derived from MyoD1- or Myf6-expressing cells or developed from a Pax7/Pax3 cell population (Relaix et al., 2005).

We are indebted to Drs Phil Soriano (Fred-Hutchinson Cancer Center, Seattle) and Eric Olson (Southwestern Medical Center, Dallas), who supplied Myf5-Cre and myogenin-Cre mice, respectively. This work was supported by the Max-Planck-Society, the DFG (ECCPS) and the European Commission (MYORES). The authors declare that they have no conflicting commercial interests related to this work.

Supplementary material

Supplementary material for this article is available at <http://dev.biologists.org/cgi/content/full/135/9/1597/DC1>

References

- Arnold, H. H. and Braun, T. (2000). Genetics of muscle determination and development. *Curr. Top. Dev. Biol.* **48**, 129–164.
- Biressi, S., Molinaro, M. and Cossu, G. (2007). Cellular heterogeneity during vertebrate skeletal muscle development. *Dev. Biol.* **308**, 281–293.
- Braun, T. and Arnold, H. H. (1994). ES-cells carrying two inactivated myf-5 alleles form skeletal muscle cells: activation of an alternative myf-5-independent differentiation pathway. *Dev. Biol.* **164**, 24–36.
- Braun, T. and Arnold, H. H. (1996). Myf-5 and myoD genes are activated in distinct mesenchymal stem cells and determine different skeletal muscle cell lineages. *EMBO J.* **15**, 310–318.
- Braun, T., Rudnicki, M. A., Arnold, H. H. and Jaenisch, R. (1992). Targeted inactivation of the muscle regulatory gene Myf-5 results in abnormal rib development and perinatal death. *Cell* **71**, 369–382.
- Brockschneider, D., Lappe-Siefke, C., Goebbels, S., Boesl, M. R., Nave, K. A. and Riethmacher, D. (2004). Cell depletion due to diphtheria toxin fragment A after Cre-mediated recombination. *Mol. Cell Biol.* **24**, 7636–7642.
- Buckingham, M. (2001). Skeletal muscle formation in vertebrates. *Curr. Opin. Genet. Dev.* **11**, 440–448.
- Buckingham, M. (2006). Myogenic progenitor cells and skeletal myogenesis in vertebrates. *Curr. Opin. Genet. Dev.* **16**, 525–532.
- Chen, Y. H., Lee, W. C., Liu, C. F. and Tsai, H. J. (2001). Molecular structure, dynamic expression, and promoter analysis of zebrafish (*Danio rerio*) myf-5 gene. *Genesis* **29**, 22–35.
- Gayraud-Morel, B., Chretien, F., Flamant, P., Gomes, D., Zammit, P. S. and Tajbakhsh, S. (2007). A role for the myogenic determination gene Myf5 in adult regenerative myogenesis. *Dev. Biol.* **312**, 13–28.
- Hasty, P., Bradley, A., Morris, J. H., Edmondson, D. G., Venuti, J. M., Olson, E. N. and Klein, W. H. (1993). Muscle deficiency and neonatal death in mice with a targeted mutation in the myogenin gene. *Nature* **364**, 501–506.
- Kablar, B., Krastel, K., Ying, C., Asakura, A., Tapscott, S. J. and Rudnicki, M. A. (1997). MyoD and Myf-5 differentially regulate the development of limb versus trunk skeletal muscle. *Development* **124**, 4729–4738.
- Kassar-Duchossoy, L., Gayraud-Morel, B., Gomes, D., Rocancourt, D., Buckingham, M., Shinin, V. and Tajbakhsh, S. (2004). Mrf4 determines skeletal muscle identity in Myf5/MyoD double-mutant mice. *Nature* **431**, 466–471.
- Kaul, A., Koster, M., Neuhaus, H. and Braun, T. (2000). Myf-5 revisited: loss of early myotome formation does not lead to a rib phenotype in homozygous Myf-5 mutant mice. *Cell* **102**, 17–19.

- Kuang, S., Kuroda, K., Le Grand, F. and Rudnicki, M. A. (2007). Asymmetric self-renewal and commitment of satellite stem cells in muscle. *Cell* **129**, 999-1010.
- Li, S., Czubryt, M. P., McAnally, J., Bassel-Duby, R., Richardson, J. A., Wiebel, F. F., Nordheim, A. and Olson, E. N. (2005). Requirement for serum response factor for skeletal muscle growth and maturation revealed by tissue-specific gene deletion in mice. *Proc. Natl. Acad. Sci. USA* **102**, 1082-1087.
- Lobe, C. G., Koop, K. E., Kreppner, W., Lomeli, H., Gertsenstein, M. and Nagy, A. (1999). Z/AP, a double reporter for cre-mediated recombination. *Dev. Biol.* **208**, 281-292.
- Ma, Q., Fode, C., Guillemot, F. and Anderson, D. J. (1999). Neurogenin1 and neurogenin2 control two distinct waves of neurogenesis in developing dorsal root ganglia. *Genes Dev.* **13**, 1717-1728.
- Megeney, L. A., Kablar, B., Garrett, K., Anderson, J. E. and Rudnicki, M. A. (1996). MyoD is required for myogenic stem cell function in adult skeletal muscle. *Genes Dev.* **10**, 1173-1183.
- Neuhaus, P. and Braun, T. (2002). Transcription factors in skeletal myogenesis of vertebrates. *Results Probl. Cell Differ.* **38**, 109-126.
- Ott, M. O., Bober, E., Lyons, G., Arnold, H. and Buckingham, M. (1991). Early expression of the myogenic regulatory gene, myf-5, in precursor cells of skeletal muscle in the mouse embryo. *Development* **111**, 1097-1107.
- Oustanina, S., Hause, G. and Braun, T. (2004). Pax7 directs postnatal renewal and propagation of myogenic satellite cells but not their specification. *EMBO J.* **23**, 3430-3439.
- Relaix, F., Rocancourt, D., Mansouri, A. and Buckingham, M. (2005). A Pax3/Pax7-dependent population of skeletal muscle progenitor cells. *Nature* **435**, 948-953.
- Rudnicki, M. A., Schnegelsberg, P. N., Stead, R. H., Braun, T., Arnold, H. H. and Jaenisch, R. (1993). MyoD or Myf-5 is required for the formation of skeletal muscle. *Cell* **75**, 1351-1359.
- Schafer, K. and Braun, T. (1999). Early specification of limb muscle precursor cells by the homeobox gene Lbx1h. *Nat. Genet.* **23**, 213-216.
- Schulze, M., Belema-Bedada, F., Technau, A. and Braun, T. (2005). Mesenchymal stem cells are recruited to striated muscle by NFAT/IL-4-mediated cell fusion. *Genes Dev.* **19**, 1787-1798.
- Soriano, P. (1999). Generalized lacZ expression with the ROSA26 Cre reporter strain. *Nat. Genet.* **21**, 70-71.
- Tajbakhsh, S. and Buckingham, M. E. (1995). Lineage restriction of the myogenic conversion factor myf-5 in the brain. *Development* **121**, 4077-4083.
- Tajbakhsh, S., Vivarelli, E., Cusella-De Angelis, G., Rocancourt, D., Buckingham, M. and Cossu, G. (1994). A population of myogenic cells derived from the mouse neural tube. *Neuron* **13**, 813-821.
- Tajbakhsh, S., Bober, E., Babinet, C., Pournin, S., Arnold, H. and Buckingham, M. (1996a). Gene targeting the myf-5 locus with nlacZ reveals expression of this myogenic factor in mature skeletal muscle fibres as well as early embryonic muscle. *Dev. Dyn.* **206**, 291-300.
- Tajbakhsh, S., Rocancourt, D. and Buckingham, M. (1996b). Muscle progenitor cells failing to respond to positional cues adopt non-myogenic fates in myf-5 null mice. *Nature* **384**, 266-270.
- Tajbakhsh, S., Rocancourt, D., Cossu, G. and Buckingham, M. (1997). Redefining the genetic hierarchies controlling skeletal myogenesis: Pax-3 and Myf-5 act upstream of MyoD. *Cell* **89**, 127-138.
- Tallquist, M. D., Weismann, K. E., Hellstrom, M. and Soriano, P. (2000). Early myotome specification regulates PDGFA expression and axial skeleton development. *Development* **127**, 5059-5070.
- Ustanina, S., Carvajal, J., Rigby, P. and Braun, T. (2007). The myogenic factor Myf5 supports efficient skeletal muscle regeneration by enabling transient myoblast amplification. *Stem Cells* **25**, 2006-2016.
- Wang, X., Blagden, C., Fan, J., Nowak, S. J., Taniuchi, I., Littman, D. R. and Burden, S. J. (2005). Runx1 prevents wasting, myofibrillar disorganization, and autophagy of skeletal muscle. *Genes Dev.* **19**, 1715-1722.

Gene Title	Gene Symbol	Probeset	Change Log Ratio	Change	Control Signal	Control Detection	Control Detection p-Value	Myf5-Cre/DT-A Signal	Myf5-Cre/DT-A Detection	Myf5-Cre/DT-A Detection p-Value	Unigene(Avadis)	Entrez	Gene	Ensembl
bone morphogenetic protein 4	Bmp4	1422912_at	0,2 NC		167,5	P	0,001953	140,5	P	0,001221	Mm.6813	12159	ENSMUSG000000021835	
desmin	Des	1426731_at	-1,3 D		263,1	P	0,000732	606,2	P	0,000244	Mm.6712	13346	ENSMUSG000000026208	
dystrophin, muscular dystrophy	Dmd	1448665_at	-0,4 NC		99,8	P	0,000244	150,6	P	0,000244	Mm.275608	13405		
dystrophin, muscular dystrophy	Dmd	1417307_at	-0,2 NC		104,5	P	0,000244	139,2	P	0,000244	Mm.275608	13405		
dystrophin, muscular dystrophy	Dmd	1430320_at	0,2 NC		10,2	P	0,000732	7	P	0,01416	Mm.275608	13405		
dystrobrevin binding protein 1	Dtnbp1	1431619_a_a	-0,1 NC		150,8	P	0,000244	155,7	P	0,000244	Mm.352311	94245	ENSMUSG000000057531	
Forkhead box P1	Foxp1	1447209_at	0,1 NC		53,6	P	0,000244	50,4	P	0,000244	Mm.234965	108655		
forkhead box P1	Foxp1	1421141_a_a	0,2 NC		94,7	P	0,000244	72,8	P	0,000244	Mm.234965	108655		
forkhead box P1	Foxp1	1435222_at	0,2 NC		297,3	P	0,000244	249,7	P	0,000244	Mm.234965	108655		
Forkhead box P1	Foxp1	1446280_at	0,3 NC		47,4	P	0,00415	38,2	P	0,001953	Mm.234965	108655		
forkhead box P1	Foxp1	1421140_a_a	0,3 NC		194,4	P	0,000244	161,7	P	0,000244	Mm.234965	108655	ENSMUSG000000030067	
forkhead box P1	Foxp1	1455242_at	0,3 NC		329,4	P	0,000244	292,7	P	0,000244	Mm.234965	108655		
Forkhead box P1	Foxp1	1438802_at	0,4 NC		46,9	P	0,000244	39,7	P	0,000244	Mm.234965	108655		
Forkhead box P1	Foxp1	1445277_at	0,4 NC		20,3	A	0,080566	15,4	P	0,030273	Mm.401795	108655		
forkhead box P1	Foxp1	1421142_s_at	0,4 NC		84,7	P	0,000244	56,1	P	0,000244	Mm.234965	108655		
forkhead box P2	Foxp2	1422014_at	-0,3 NC		27,3	A	0,067627	24,9	P	0,01416	Mm.432481	114142	ENSMUSG000000029563	
forkhead box P2	Foxp2	1441365_at	-0,2 NC		16,4	P	0,005859	22,5	P	0,00415		114142		
forkhead box P2	Foxp2	1458191_at	-0,2 NC		34,4	P	0,000244	44,1	P	0,000244	Mm.432481	114142		
forkhead box P2	Foxp2	1440108_at	-0,2 NC		84,8	P	0,000732	86,7	P	0,000244	Mm.432481	114142	ENSMUSG000000029563	
forkhead box P2	Foxp2	1438232_at	-0,1 NC		161,1	P	0,000244	160,5	P	0,000244	Mm.432481	114142	ENSMUSG000000029563	
forkhead box P2	Foxp2	1438231_at	0,1 NC		96,2	P	0,000244	88,4	P	0,000244	Mm.432481	114142	ENSMUSG000000029563	
Follistatin	Fst	1434458_at	-0,1 NC		113,6	P	0,000244	120,4	P	0,000244	Mm.425842	14313		
folistatin	Fst	1421365_at	0,1 NC		99,5	P	0,023926	95,7	P	0,023926	Mm.425842	14313	ENSMUSG000000021765	
lectin, galactose binding, soluble 1	Lgals1	1455439_a_a	0 NC		4727	P	0,000244	4785,7	P	0,000244	Mm.43831	16852	ENSMUSG000000068220	
lectin, galactose binding, soluble 1	Lgals1	1419573_a_a	0 NC		2655,3	P	0,000244	2902,7	P	0,000244	Mm.43831	16852	ENSMUSG000000068220	
muscleblind-like 1 (Drosophila)	Mbnl1	1440315_at	-0,2 NC		6	P	0,010742	7	P	0,008057	Mm.255723	56758		
muscleblind-like 1 (Drosophila)	Mbnl1	1416904_at	0 NC		1084	P	0,000244	1078,9	P	0,000244		56758	ENSMUSG000000027763	
Muscleblind-like 3 (Drosophila)	Mbnl3	1442664_at	-0,3 NC		11,1	P	0,030273	11	P	0,005859	Mm.295324	171170		
muscleblind-like 3 (Drosophila)	Mbnl3	1422836_at	0,1 NC		87,1	P	0,001221	70,8	P	0,000244	Mm.295324	171170		
muscleblind-like 3 (Drosophila)	Mbnl3	1434678_at	0,1 NC		271	P	0,000244	243,6	P	0,000244	Mm.295324	171170		
Muscleblind-like 3 (Drosophila)	Mbnl3	1441530_at	0,5 NC		28,6	P	0,010742	18,4	M	0,056152	Mm.295324	171170		
Muscleblind-like 3 (Drosophila)	Mbnl3	1443383_at	0,5 NC		22,6	P	0,001953	22,3	P	0,001221	Mm.295324	171170		
muscleblind-like 3 (Drosophila)	Mbnl3	1442549_at	0,6 NC		74,3	P	0,001221	58,8	P	0,005859	Mm.295324	171170		
myocyte enhancer factor 2C	Mef2c	1451507_at	-1 D		144,7	P	0,000732	299	P	0,000244	Mm.428347	17260		
myocyte enhancer factor 2C	Mef2c	1424852_at	-0,9 NC		243,7	P	0,000732	441,6	P	0,000244	Mm.428347	17260		
myocyte enhancer factor 2C	Mef2c	1421027_a_a	-0,8 NC		332,5	P	0,000244	588,4	P	0,000244	Mm.24001	17260	ENSMUSG000000005583	
myocyte enhancer factor 2C	Mef2c	1451506_at	-0,7 NC		182,8	P	0,005859	373,3	P	0,000244	Mm.24001	17260		
myocyte enhancer factor 2C	Mef2c	1421028_a_a	-0,7 NC		167	P	0,000244	271	P	0,000244	Mm.24001	17260	ENSMUSG000000005583	
Myocyte enhancer factor 2C	Mef2c	1439946_at	-0,4 NC		39,7	P	0,008057	55,7	P	0,001953	Mm.24001	17260		
Myocyte enhancer factor 2C	Mef2c	1445420_at	-0,4 NC		29,5	P	0,000732	34,2	P	0,000244	Mm.24001	17260		
Myocyte enhancer factor 2C	Mef2c	1446484_at	-0,2 NC		56,6	P	0,001221	65,1	P	0,001221	Mm.24001	17260		
homeo box, msh-like 1	Msx1	1448601_s_at	0,2 NC		40,8	P	0,001953	37,5	P	0,023926	Mm.256509	17701	ENSMUSG000000048450	
myogenic factor 5	Myf5	1420757_at	-1,5 D		8,8	A	0,080566	42,5	P	0,000244	Mm.4984	17877	ENSMUSG000000000435	
myogenic factor 6	Myf6	1419150_at	-1,8 D		33,8	P	0,008057	146,4	P	0,000732	Mm.11	17878	ENSMUSG0000000035923	
myogenic differentiation 1	Myod1	1418420_at	-0,5 NC		106,5	P	0,010742	157,2	P	0,001953	Mm.1526	17927	ENSMUSG000000009471	
myogenin	Myog	1419391_at	-0,8 NC		294	P	0,000244	465,5	P	0,000244	Mm.16528	17928	ENSMUSG000000026459	
myomesin 2	Myom2	1438175_x_at	-1,5 D		75,7	P	0,001221	266,2	P	0,000732	Mm.272115	17930	ENSMUSG000000031461	
myomesin 2	Myom2	1457435_x_at	-1,4 D		358,1	P	0,000244	948,7	P	0,000244	Mm.272115	17930	ENSMUSG000000031461	
myomesin 2	Myom2	1450917_at	-1,4 D		134,2	P	0,008057	355,2	P	0,000732	Mm.272115	17930	ENSMUSG000000031461	
Neurofibromatosis 1	Nf1	1460055_at	0 NC		9,9	P	0,046143	7,1	P	0,001953	Mm.255596	18015		
neurofibromatosis 1	Nf1	1438067_at	0,4 NC		56,4	P	0,001953	45,2	P	0,00293		18015	ENSMUSG000000020716	
Neurofibromatosis 1	Nf1	1443894_at	0,5 NC		43,5	P	0,01416	34,6	P	0,01416	Mm.255596	18015		
p21 (CDKN1A)-activated kinase 1	Pak1	1420979_at	-0,3 NC		81	P	0,000732	90,2	P	0,000732	Mm.260227	18479	ENSMUSG000000030774	
p21 (CDKN1A)-activated kinase 1	Pak1	1420980_at	-0,1 NC		95	P	0,000732	104,5	P	0,000244	Mm.260227	18479	ENSMUSG000000030774	
p21 (CDKN1A)-activated kinase 1	Pak1	1450070_s_at	0,1 NC		132	P	0,000244	136,7	P	0,000732	Mm.260227	18479	ENSMUSG000000030774	
PDZ and LIM domain 3	Pdlim3	1449178_at	-0,9 NC		258,1	P	0,001953	502,9	P	0,000732	Mm.282900	53318	ENSMUSG000000031636	
PDZ and LIM domain 3	Pdlim3	1443299_at	-0,8 NC		66,3	P	0,000244	144,6	P	0,000244	Mm.282900	53318		
protein phosphatase 3, catalytic subunit, alpha isoform	Ppp3ca	1452056_s_at	-0,2 NC		170,5	P	0,000244	186	P	0,000244	Mm.331389	19055	ENSMUSG000000028161	
protein phosphatase 3, catalytic subunit, alpha isoform	Ppp3ca	1426401_at	-0,1 NC		281,6	P	0,000244	313,4	P	0,000244	Mm.331389	19055	ENSMUSG000000028161	
protein phosphatase 3, catalytic subunit, alpha isoform	Ppp3ca	1438478_a_a	-0,1 NC		172,6	P	0,000732	217	P	0,000244	Mm.331389	19055	ENSMUSG000000028161	
Protein phosphatase 3, catalytic subunit, alpha isoform	Ppp3ca	1440051_at	0,2 NC		58,1	P	0,000244	48,3	P	0,000732	Mm.331389	19055		
ras homolog gene family, member A	Rhoa	1437628_s_at	0,1 NC		951	P	0,000244	887,9	P	0,000244	Mm.757	11848	ENSMUSG000000007815	
sonic hedgehog	Shh	1436869_at	-0,6 NC		121,7	P	0,000244	240,8	P	0,000732	Mm.57202	20423	ENSMUSG00000002633	
sine oculis-related homeobox 1 homolog (Drosophila)	Six1	1427277_at	-0,8 NC		24,6	P	0,000244	51,5	P	0,000244	Mm.4645	20471	ENSMUSG000000051367	
sine oculis-related homeobox 4 homolog (Drosophila)	Six4	1456862_at	-0,6 NC		21,3	P	0,00415	43,4	P	0,000732	Mm.249575	20474		
sine oculis-related homeobox 4 homolog (Drosophila)	Six4	1425767_a_a	-0,2 NC		50,4	P	0,001953	59,4	P	0,001953	Mm.249575	20474	ENSMUSG0000000034460	
sine oculis-related homeobox 4 homolog (Drosophila)	Six4	1439753_x_at	-0,2 NC		26,8	P	0,010742	38,8	P	0,001221	Mm.249575	20474		
serum response factor	Srf	1418255_s_at	-0,6 NC		124,2	P	0,000244	170,7	P	0,000244	Mm.45044	20807	ENSMUSG000000015605	
serum response factor	Srf	1418256_at	-0,1 NC		112,2	M	0,056152	126,1	P	0,023926	Mm.45044	20807	ENSMUSG000000015605	
serine/arginine-rich protein specific kinase 3	Srpk3	1447806_s_at	-1 NC		201,7	P	0,00415	388,2	P	0,00293	Mm.111904	56504	ENSMUSG000000002007	
serine/arginine-rich protein specific kinase 3	Srpk3	1418798_s_at	-0,7 NC		108	P	0,00293	209,8	P	0,000244	Mm.111904	56504	ENSMUSG000000002007	
T-box 1	Tbx1	1425779_a_a	-0,3 NC		40,8	M	0,056152	50,1	P	0,030273	Mm.295194	21380	ENSMUSG000000009097	
transforming growth factor, beta 1	Tgfb1	1420653_at	0 NC		153,3	P	0,005859	158,3	P	0,001953	Mm.248380	21803	ENSMUSG000000002603	
vestigial like 2 homolog (Drosophila)	Vgll2	1436361_at	-0,7 NC		186,2	P	0,001953	254	P	0,001953	Mm.87237	215031	ENSMUSG000000049641	